Microsecond Model Updating for 2D Structural Systems Using the Local Eigenvalue Modification Procedure

EMMANUEL A. OGUNNIYI, ALEXANDER B. VEREEN
and AUSTIN R. J. DOWNEY

ABSTRACT

Systems that experience high-rate dynamics, such as blast or impact, are susceptible to rapid alterations that could result in loss of life and financial investments. These systems are characterized by a high dynamic response with a high-rate (< 100 ms) and high amplitude (> 100 g_s). A system exposed to high-rate dynamic environments is frequently prone to rapid plastic deformation, which can cause structural, electrical, and sensor damage. A feedback loop of fast-acting actuators empowered with rapid state estimates can be utilized to stop further harm. The state estimator must be quick and resilient to the significant uncertainties, non-stationarities, and strong disturbances associated with high-rate dynamic systems. A model for 2Dimensional systems is developed to demonstrate high-rate tracking or estimation of a structure where a change in stiffness at locations on the system represents damage. The Local Eigenvalue Modification Procedure (LEMP) algorithm is applied to solve the system's equation quickly and efficiently within a set latency for state estimation. LEMP utilizes a single generalized eigenvalue solution for the initial system and simplifies altered state equations by transforming them into modal space, isolating the DOFs that contribute to the changes between states, and defining equations in terms of the initial state, thereby reducing computational time. This preliminary work develops a 2D finite element model using classical plate theory. A 2D model simulation of the plate's initial state is carried out on Abaqus and compared to the analytical model formulated solved using the generalized eigenvalue approach to test the formulated model. The changes made to the plate are then solved using LEMP to avoid solving the time-consuming eigenvalue solution. In this work, the change in the system is demonstrated by change in stiffness at different locations on the plate. Results report the performance metrics for the considered case. The approach's applicability to deployment on edge computing systems for real-time model updating of structures operating in high-rate dynamic environments is discussed.

Emmanuel A. Ogunniyi, Alexander B. Vereen, Department of Mechanical Engineering, University of South Carolina, Columbia, SC, USA
Austin R.J. Downey, Assistant Professor, Email: austindowney@sc.edu Department of Mechanical, Civil, and Environmental Engineering, University of South Carolina, Columbia, SC, USA

INTRODUCTION

High-rate structural dynamics is a field of study concerned with the response of structures to dynamic loading at high high-amplitude accelerations (> 100 g_n) and occur at high-rates ($<$100 ms) such as those experienced during impacts, explosions, or seismic events. The behavior of structures under these extreme conditions can be significantly different from their response under static or low-rate loading [1]. This makes it essential to understand the behavior of structures under high-rate loading to design safe and reliable structures that can withstand extreme events. These events are complex and unpredictable, as the loading conditions on the structure change abruptly and unexpectedly, altering the internal and external forces experienced by the system. As a result, tracking the state of the structure throughout the event poses a significant challenge due to the sudden and uncertain nature of the changes. High-rate structural dynamics has numerous applications, including designing protective structures, such as blast-resistant buildings and nuclear power plants, and developing new materials for high-speed transportation systems. [2, 3].

Model updating is essential for ensuring the safety and integrity of structures, especially those subject to dynamic loads and uncertain environmental conditions. Model updating can be either data-driven or model-based. For example, Samte et al. in [4] deployed LSTM models in real-time, a data-driven approach for high-rate state estimation. Downey et al. also applied a model-based approach to update the state of high-rate dynamic events generated on the DROPBEAR experimental testbed [5]. Model-driven real-time control of structures operating in high-rate dynamic environments requires models updated on the microsecond timescale. Model updating is a critical process in model-driven structural control as the model determines the control decisions to be executed by the active structures. Without model updating, the control system may not function as expected, leading to reduced effectiveness in mitigating vibrations or preventing damage to the structure.

The local eigenvalue modification procedure method simplifies a system state calculations by truncating the number of independent systems with a single degree of freedom to include only the most significant modes [6, 7]. Doing so transforms the generalized eigenvalue equation into a set of second-order equations that can be solved based on the system's initial frequencies. This reduces the number and complexity of equations required to determine the structure's state, leading to faster computation times. The LEMP approach is advantageous because it does not require solving the generalized eigenvalue problem, making it a more efficient method for calculating the dynamic response of a structure.

The authors previously used LEMP to solve the system's equation for a 1D system undergoing a single change [8, 9]. In this work, the authors investigate the performance of LEMP on 2D systems formulated using the Mindlin plate theory. The LEMP algorithm is used alongside the generalized eigenvalue procedure to calculate the change in frequency when a single change is applied to the system. The contributions of this work are 1) formulation of a model for a 2D system, 2) applying LEMP to solve for a single change in the system, and 3) evaluation of the performance of LEMP against GE using the error and time as criteria.

METHODOLOGY

The 2D model is created by employing the Mindlin plate theory to develop shell elements for rectangular plates. This involves superposing a 2D solid element onto a 2D plate element. The solid element addresses in-plane effects like membrane behavior, and the plate element manages off-plane effects like bending. Figure 1 shows the shell element formation and its coordinate system, where Figure 1(a) shows how an element is broken into nodes, Figure 1(b) and (c) shows the coordinate system of a 2D solid element with 2 DOFs. Figure 1(d) depicts a plate structure, and Figure 1(e) is the shell coordinate system that combines the 2D solid element and plate structure.

The 2D plate model development process can be summarized into Three steps:

1. Construction of shape functions matrix **N** that satisfies Eqs. 1
2. Formulation of the strain matrix for 2D element **B**, Eq. 3 and 2D plate, $\mathbf{B}^{\mathrm{I}}$ and $\mathbf{B}^{\mathbf{O}}$ shown in Eqs. 4 and 5.
3. Calculation of $\mathbf{k}_e$ and $\mathbf{m}_e$ using shape functions **N** and strain matrix in step 2 to obtain Eqs. 5 and 6.

Step 1: Construction of shape functions for the 2D elements and plate is obtained in Eq. 1 where $\mathbf{N}_e$ is shape function for 2D element and $\mathbf{N}_p$ is for 2D plate. This study uses the Mindlin plate theory to develop rectangular elements for the 2D plate. When analyzing the plate structure, it is assumed that the element has a uniform thickness, denoted as h.

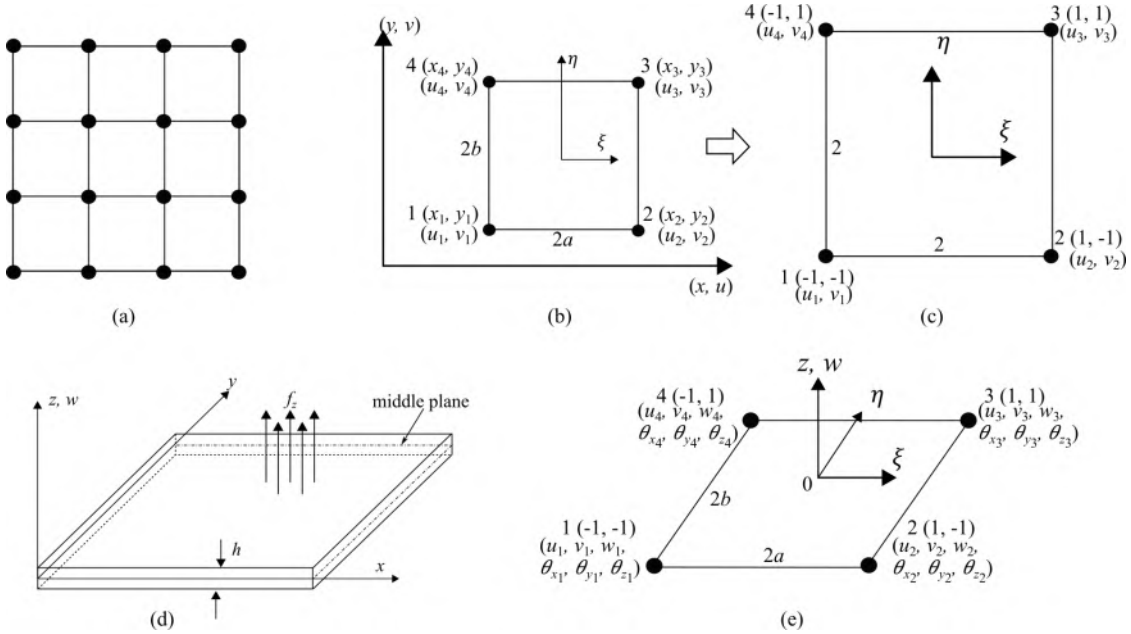

Figure 1. Shell element formation and its coordinate system where; (a) represents the nodal construction on the element; (b) shows the coordinate system of a 2D solid element with 2 DOFs; (c) shows the transformation of the coordinate system with dimension; (d) depicts a plate structure, and; (e) is the shell coordinate system that combines the 2D solid element and plate structure.

$$\mathbf{N}_e = \begin{bmatrix} N_1 & 0 & N_2 & 0 & N_3 & 0 & N_4 & 0 \\ 0 & N_1 & 0 & N_2 & 0 & N_3 & 0 & N_4 \end{bmatrix} \tag{1}$$

$$\mathbf{N}_p = \begin{bmatrix} N_1 & 0 & 0 & N_2 & 0 & 0 & N_3 & 0 & 0 & N_4 & 0 & 0 \\ 0 & N_1 & 0 & 0 & N_2 & 0 & 0 & N_3 & 0 & 0 & N_4 & 0 \\ 0 & 0 & N_1 & 0 & 0 & N_2 & 0 & 0 & N_3 & 0 & 0 & N_4 \end{bmatrix} \tag{2}$$

Step 2: Formulation of the strain matrix **B**. The 2D solid element has one strain matrix Eq. 3, while the 2D solid plate has two strain, $\mathbf{B}_{\mathrm{I}}$ and $\mathbf{B}_{\mathrm{O}}$ as shown in Eqs. 4 and 5. The strain matrix $\mathbf{B}_{\mathrm{I}}$ represents the strain energy associated with the in-plane stress and strain while $\mathbf{B}_{\mathrm{O}}$ relates to the strain energy associated with the off-plane shear stress and strain.

$$\mathbf{B} = \mathbf{L}\mathbf{N} = \frac{1}{4}\begin{bmatrix} -\frac{1-\eta}{a} & 0 & \frac{1-\eta}{a} & 0 & \frac{1+\eta}{a} & 0 & -\frac{1+\eta}{a} & 0 \\ 0 & -\frac{1-\xi}{b} & 0 & -\frac{1+\xi}{b} & 0 & \frac{1+\xi}{b} & 0 & \frac{1-\xi}{b} \\ -\frac{1-\xi}{b} & -\frac{1-\eta}{a} & -\frac{1+\xi}{b} & \frac{1-\eta}{a} & \frac{1+\xi}{b} & \frac{1+\eta}{a} & \frac{1-\xi}{b} & -\frac{1+\eta}{a} \end{bmatrix} \tag{3}$$

$$\mathbf{B}^{\mathrm{I}} = \begin{bmatrix} \mathbf{B}_1^{\mathrm{I}} & \mathbf{B}_2^{\mathrm{I}} & \mathbf{B}_3^{\mathrm{I}} & \mathbf{B}_4^{\mathrm{I}} \end{bmatrix}, \qquad \mathbf{B}_{\mathrm{j}}^{\mathrm{I}} = \begin{bmatrix} 0 & 0 & -\partial N_j/\partial x \\ 0 & \partial N_j/\partial x & 0 \\ 0 & \partial N_j/\partial y & -\partial N_j \partial y \end{bmatrix} \tag{4}$$

$$\mathbf{B}^{\mathrm{O}} = \begin{bmatrix} \mathbf{B}_1^{\mathrm{O}} & \mathbf{B}_2^{\mathrm{O}} & \mathbf{B}_3^{0} & \mathbf{B}_4^{0} \end{bmatrix}, \qquad \mathbf{B}_{\mathrm{j}}^{\mathrm{O}} = \begin{bmatrix} \partial N_j/\partial x & 0 & N_j \\ \partial N_j/\partial y & -N_j & 0 \end{bmatrix} \tag{5}$$

This work uses a plate represented by a two-dimensional domain in the $x-y-z$ plane, as shown in Figure1(d). As depicted in Figure1(a), the plate has been divided into rectangular sections appropriately. Each of these sections comprises four nodes and four straight edges. At a node, the degrees of freedom (DOFs) include the deflection u, v, and w, as well as the rotation about the x-axis (θ_x), y-axis (θ_y) and z-axis (θ_z), resulting in a total of six DOFs per node. Thus, for a rectangular section with four nodes, the total number of DOFs for that section would be 24.

Step 3: Calculation of $\mathbf{k}_e$ and $\mathbf{m}_e$ using shape functions N and strain matrix to obtain Eqs. 6 and 7.

The element matrices can be obtained using the shape function and nodal variables. Similar matrices can be obtained for 2D elements and plates; however, in 2D plates, 3 DOFs are used for defining the system, while 2 DOFs are used for the 2D element. The mass and stiffness matrices can be obtained using the energy functions, and Hamilton's principle described in Liu et al. [10]. Eq 6 is the mass matrix where I is a diagonal matrix.

TABLE I. MATERIAL PROPERTIES

Type	Poisson's ratio	Young's modulus	density	thickness
steel	0.3	200e9	7700 kg/m^3	0.006 m

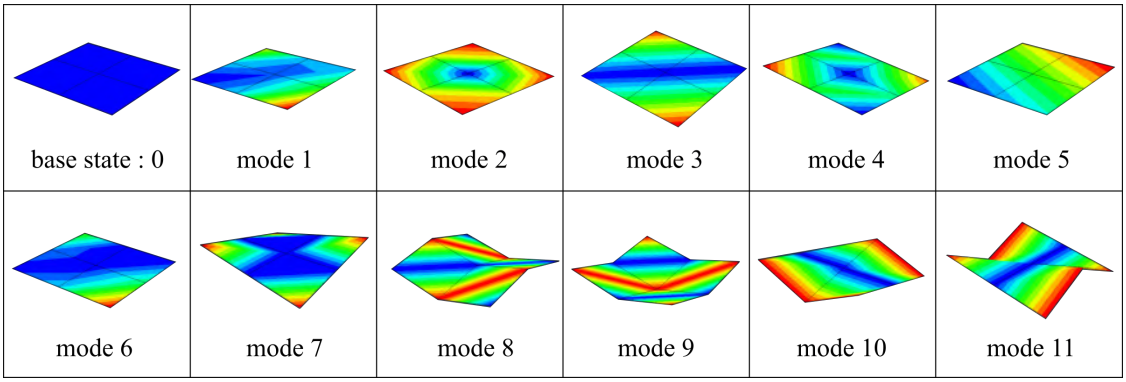

Figure 2. Mode shapes of a 2D plate shown in figure 1.

$$\mathbf{I} = \begin{bmatrix} \rho h & 0 & 0 \\ 0 & \rho h^3/12 & 0 \\ 0 & 0 & \rho h^3/12 \end{bmatrix}, \qquad \mathbf{m}_{\mathrm{e}} = \int_A h\rho \mathbf{N}^{\mathrm{T}}\mathbf{N}\mathrm{dA}, \qquad \mathbf{m}_{\mathrm{p}} = \int_{A_p} \mathbf{N}^{\mathrm{T}}\mathbf{I}\mathbf{N}\mathrm{dA} \tag{6}$$

where ρ and h are the density and thickness of the plate respectively.

$$\mathbf{k}_{\mathrm{e}} = \int_A h\mathbf{B}^{\mathrm{T}}\mathbf{c}\mathbf{B}\mathrm{dA}, \qquad \mathbf{k}_{\mathrm{p}} = \int_{A_p} \frac{h^3}{12} \left[\mathbf{B}^{\mathrm{I}}\right]^{\mathrm{T}} \mathbf{c}\mathbf{B}^{\mathrm{I}} dA + \int_{A_p} \kappa h \left[\mathbf{B}^{\mathrm{O}}\right]^{\mathrm{T}} \mathbf{c}_s \mathbf{B}^{\mathrm{O}} dA \tag{7}$$

The integration in the stiffness matrix $\mathbf{k}_{\mathrm{e}}$, can be evaluated analytically, however, the Gauss integration scheme is used to evaluate the integration numerically.

To validate the 2D model formulated above, a frequency analysis of a 2D system was conducted using Abaqus. The analysis was carried out according to the following procedure:

First, a 2D plate model is created, which includes defining the plate's geometry, thickness, and material properties based on Table I. For preliminary validation of the model, no boundary conditions were defined. Material properties such as density, Young's modulus, and Poisson's ratio were assigned to the plate material to enable accurate simulation of the plate's mechanical behavior. The plate was meshed using finite element analysis techniques built in Abaqus. In this analysis, only four elements were generated, corresponding to nine nodes and 54 DOFs on the plate. The frequency range of interest was set to a maximum of 2000 Hz. The frequency and mode shapes of the model were then generated, with the first elastic mode of the plate observed at mode 7, with a frequency of 232 Hz. The simulated results for each mode up to mode 12 were shown in Figure 2.

TABLE II. BASE STATE FREQUENCY EXTRACTION

mode	7	8	9	10	11	12
Abaqus	232.12	378.77	515.89	598.64	594.64	944.72
Generalized Eigenvalue	232.027	379.044	515.983	598.768	598.768	945.03
error (abs)	0.093	0.274	0.0093	0.128	4.128	0.31

The formulated 2D model's initial state (base state) frequencies were calculated using the generalized eigenvalue approach. The frequencies from the simulated model (Abaqus) and the GE at modes 7 to 11 were then compared and tabulated in Table II. The system frequencies were calculated with the generalized eigenvalue approach closely aligned with those from the Abaqus model. The low error between both frequencies obtained indicates that the 2D model developed is correct.

RESULTS

A local change is applied to a 9-node plate as a form of increased stiffness at the nodes. Before a stiffness change is applied at each node, the four corners of the plate

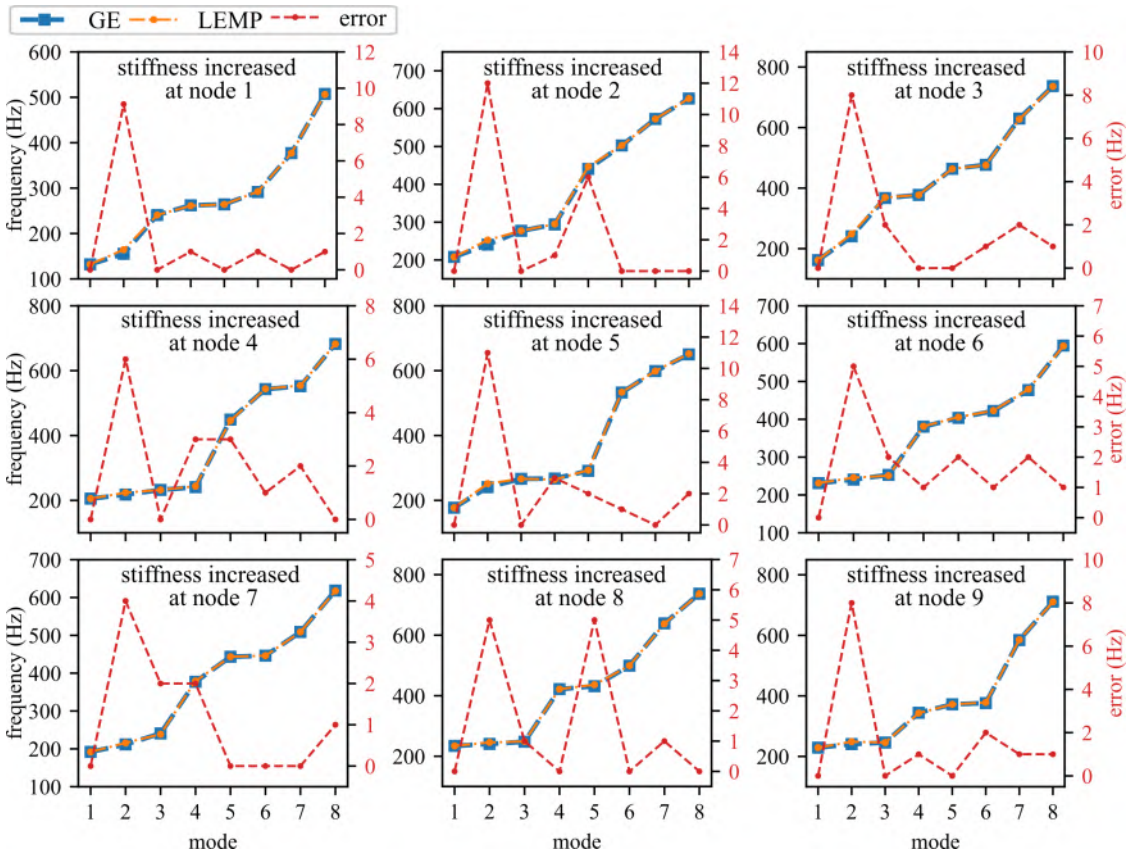

Figure 3. Frequency of the first eight modes of the 2D plate for a change of 1e100 N/m stiffness introduced to the system at one of he nine nodes in the system. The frequency response of the system is calculated using both GE and LEMP and the error between the two is reported.

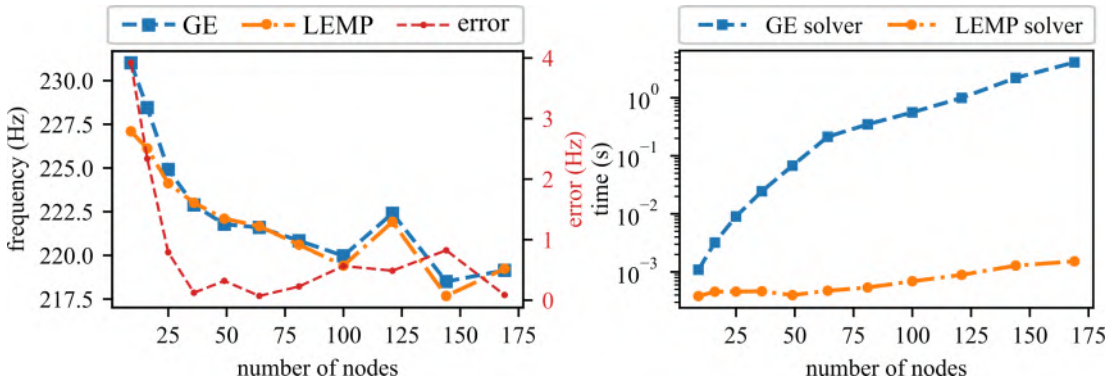

Figure 4. Frequency response calculated for: (a) the first elastic mode using GE and LEMP on a plate of 9 nodes up to 169 nodes as tabulated in table III, and; (b) time taken to solve the system equation at each number of nodes tested shown in Table III.

are fixed by increasing the stiffness by 5e100 N/m of both the deflection and rotation on the z-axis. This nodal change is then applied at at each node, from node 1 to 9. The first eight modal frequencies are obtained using generalized eigenvalue and LEMP approaches. The performance of the LEMP algorithm compared to the generalized eigenvalue procedure on the 2D system is recorded. Figure 3 shows similarity in frequencies calculated using both approaches for nodes 1-9. A notable change in frequency is only observed in the second mode, where the error value is higher than at other modes; however, the difference is less than 10 Hz at most nodes.

The generalized eigenvalue and LEMP solver were also tested on 2D plates with increasing numbers of nodes numbers of nodes. As opposed to the 1-D system, where the matrix of the system grows gradually, the 2D system grows exponentially quicker as the system has 6 DOFs per node in the 2D system compared to just 2 DOFs in the 1-D system. To expand, the system matrix is 54 $\times$ 54 as compared to 18 $\times$ 18 for a 1-D system. Also, at 100 nodes, the 2D system has a matrix of size 600 $\times$ 600, whereas the 1-D system has a size 200 $\times$ 200. Table III reports how the matrix size grows as the number of nodes increases. This matrix size growth also shows the need for a faster algorithm for solving the system equation. The first elastic mode frequency calculated using GE

TABLE III. SINGLE STATE CHANGE CALCULATED USING THE LEMP AND GENERALIZED EIGENVALUE PROCESS

single change calculated using:				generalized eigenvalue		LEMP		
no. of nodes	no. of element	DOF	matrix size	freq (Hz)	time GE (s)	freq (Hz)	time LEMP (s)	error (Hz)
9	4	54	54 x 54	232.027	0.001093	227.099	0.000384	4.928
16	9	96	96 x 96	228.458	0.00320	226.120	0.000456	2.338
25	16	150	150 x 150	224.914	0.009031	224.123	0.000458	0.791
36	25	216	216 x 216	222.886	0.024529	223.01	0.000464	-0.124
49	36	294	294 x 294	221.78	0.067579	222.1	0.000399	-0.32
64	49	384	384 x 384	221.599	0.212773	221.67	0.000475	-0.071
81	64	486	486 x 486	220.837	0.348656	220.610	0.000539	0.227
100	81	600	600 x 600	219.975	0.559744	219.41	0.000691	0.565
121	100	726	726 x 726	222.409	0.994675	221.919	0.000890	0.488
144	121	864	864 x 864	218.505	2.197694	217.68	0.001285	0.825
169	144	1014	1014 x 1014	219.147	4.075451	219.234	0.001523	-0.087

and LEMP for nine nodes up to 169 nodes is shown in Figure 4(a). A closer frequency value between the two approaches is achieved as the number of nodes increases. The system equation solving time is expanded upon in Figure 1(b). Up to 100 nodes, the LEMP algorithm can still achieve 691 μs while GE is already at 0.56 s. At 169 nodes, the LEMP algorithm stands at 1.5 ms and the GE at 4 s which defiles the microsecond constraint investigated.

CONCLUDING REMARKS

This work demonstrated the potential of using the local eigenvalue modification procedure (LEMP) to estimate the state of a 2D system formulated using the Mindlin plate theory. The model developed accuracy was compared to 2D shell simulation on Abaqus, where the base state frequencies obtained were compared to ones from the generalized eigenvalue approach. A nine-node 2D element is then used to investigate the performance and timing of the LEMP process for a single-state change in the system. A singular change is applied to the system in the form of a change in stiffness at each node from one to nine, and the corresponding change in frequencies due to the change is calculated using GE and LEMP. The obtained frequencies from both approaches were close; however, the timing performance is different. As the system matrix grows, the GE fails the time constraint, while the LEMP still achieves a single state change update of 1.5 ms at 169 nodes.

ACKNOWLEDGMENT

This material is based upon work supported by the Air Force Office of Scientific Research (AFOSR) through award no. FA9550-21-1-0083. This work is also partly supported by the National Science Foundation grant numbers 1850012, 1937535, and 1956071. This material is partially based upon work supported by the University of South Carolina through grant number 80003212. Any opinions, findings, and conclusions or recommendations expressed in this material are those of the authors and do not necessarily reflect the views of the University of South Carolina, the National Science Foundation, or the United States Air Force.

REFERENCES

1. Hong, J., S. Laflamme, J. Dodson, and B. Joyce. 2018. “Introduction to State Estimation of High-Rate System Dynamics,” *Sensors*, 18(2):217, doi:10.3390/s18010217.
2. Mostert, F. 2018. “Challenges in blast protection research,” *Defence Technology*, 14(5):426–432, doi:10.1016/j.dt.2018.05.007.
3. Richert, J., D. Coutellier, C. Götz, and W. Eberle. 2007. “Advanced smart airbags: The solution for real-life safety?” *International Journal of Crashworthiness*, 12(2):159–171, doi:10.1080/13588260701433461.
4. Satme, J., D. Coble, B. Priddy, A. R. J. Downey, J. D. Bakos, and G. Comert. 2022. “Progress Towards Data-Driven High-Rate Structural State Estimation on Edge Computing Devices,”

in *Volume 10: 34th Conference on Mechanical Vibration and Sound (VIB)*, American Society of Mechanical Engineers, doi:10.1115/detc2022-90118.

5. Downey, A., J. Hong, J. Dodson, M. Carroll, and J. Scheppegrell. 2020. "Millisecond model updating for structures experiencing unmodeled high-rate dynamic events," *Mechanical Systems and Signal Processing*, 138:106551, doi:10.1016/j.ymssp.2019.106551.
6. Weissenburger, J. T. 1968. "Effect of Local Modifications on the Vibration Characteristics of Linear Systems," *Journal of Applied Mechanics*, 35(2):327–332, doi:10.1115/1.3601199.
7. Sestieri, A. 2000. "Structural dynamic modification," *Sadhana*, 25(3):247–259, doi:10.1007/bf02703543.
8. Ogunniyi, E., A. R. J. Downey, and J. Bakos. 2022. "Development of a real-time solver for the local eigenvalue modification procedure," SPIE, ISBN 9781510649675, p. 51, doi:10.1117/12.2613208.
9. Ogunniyi, E. A., C. Drnek, S. H. Hong, A. R. Downey, Y. Wang, J. D. Bakos, P. Avitabile, and J. Dodson. 2023. "Real-time structural model updating using local eigenvalue modification procedure for applications in high-rate dynamic events," *Mechanical Systems and Signal Processing*, 195:110318, doi:10.1016/j.ymssp.2023.110318.
10. Liu, G. and S. Quek. 2014. "Chapter 8 - FEM for Plates and Shells," in G. Liu and S. Quek, eds., *The Finite Element Method (Second Edition)*, Butterworth-Heinemann, Oxford, second edition edn., ISBN 978-0-08-098356-1, pp. 219–247, doi:https://doi.org/10.1016/B978-0-08-098356-1.00008-4.